JOURNAL OF CATALYSIS **171,** 14–26 (1997)
ARTICLE NO. CA971768

Kinetic and Mechanistic Study of NO_x Reduction by NH_3 over H-Form Zeolites

I. Kinetic and Mechanistic Insights into NO Reduction over H-ZSM-5

John Eng and Calvin H. Bartholomew

BYU Catalysis Laboratory, Brigham Young University, Provo, Utah 84602

Received August 12, 1996; revised March 27, 1997; accepted June 4, 1997

A study of the kinetics and mechanism of the selective catalytic reduction (SCR) of NO by NH_3 over H-ZSM-5 was undertaken. Steady-state kinetic experiments performed at temperatures above 330°C with and without the presence of H_2O indicate that H_2O does not affect SCR by NH_3 at these temperatures. Analysis of the kinetic data indicates that SCR is positive order in NO and O_2 and inhibited by NH_3. A series of transient tests were also performed to determine the roles of NO, O_2, and NH_3 in the mechanism of NO SCR. Transient test results indicate that O_2 reacts with NO to form an active intermediate species (possibly NO_2 or NO^+) which reacts with adsorbed NH_3. Transient test results also suggest that although adsorbed NH_3 is necessary for NO reduction to proceed, excess gaseous NH_3 inhibits SCR. Comparisons of SCR activity exhibited by samples of H-ZSM-5 and H-mordenite of different Si/Al ratios suggest that a limiting Al content is necessary for H-form zeolites to be active. This result suggests that pairs of neighboring Brønsted acid sites are necessary for adsorption of NH_3, such that the adsorbed NH_3 molecules are close enough together that they can both bond with other reactant molecules.

INTRODUCTION

Increasingly stringent NO_x emissions standards have stimulated the development of more active NO_x reduction catalysts.

Pence and Thomas (1) first documented the activity of H-mordenite as a catalyst for selectively reducing NO_x to N_2 using NH_3 as a reducing agent and thus created interest in the use of zeolites as selective catalytic reduction (SCR) catalysts. Developments by Kiovsky and co-workers (2), resulting in the production of a commercial Fe-H-mordenite catalyst (NC-300), further stimulated this interest. In the same time frame, Seiyama and co-workers (3) investigated the SCR activity of various transition metal ion-exchanged Y zeolite catalysts. Promising results led to a variety of studies focusing on the enhancement in SCR activity achieved by exchanging metals (e.g., Fe, Cu, Ni, Pt, Rh, Co, Ga, etc.) into different zeolites (e.g., Y, mordenite, ZSM-5, ferrierite, beta zeolites). Based upon these studies, it is evident that proper selection of metals exchanged into appropriate zeolites can greatly enhance the activity of SCR catalysts. It is interesting to note, however, that the SCR activity and selectivity of these same metals significantly decrease unless the metals are exchanged into appropriate zeolites. Conversely, studies have confirmed that these same zeolites in their metal-free form (H-form) are active SCR catalysts (4–7). This, it is clear that the zeolite is much more than just a high-surface-area physical support for the metal. Nevertheless, little fundamental work has been performed to elucidate the kinetics and mechanisms of SCR on H-form zeolites.

Analysis of reported experimental NO_x conversions obtained over metal-exchanged and H-form zeolites reveals interesting similarities. Brandin *et al.* (6) and Ham *et al.* (7) presented results of NO conversions for Cu-exchanged, Fe-exchanged, and H-form mordenite using NH_3 as a reducing agent. Their results show that Cu-mordenite is capable of achieving 100% NO conversion at approximately 250°C, while H-mordenite requires temperatures above 400°C. It is interesting to note, however, that the conversion–temperature profiles for each of these catalysts have very similar shapes, differing only in a temperature offset. Experiments performed by Yogo and co-workers (8), using CH_4 as a reducing agent, demonstrate that conversion–temperature profiles obtained for H-ZSM-5 are bell shaped with a maximum conversion between 40 and 50% at approximately 500°C. In comparison, Li and Armor (9) presented similar conversion–temperature profiles for Co-ZSM-5 with a maximum NO conversion close to 50% occurring at just over 400°C (GHSV similar to that used in work of Yogo and co-workers). The similarity of conversion–temperature profiles in metal-exchanged and H-form zeolites suggests that metals enhance certain rate-limiting reaction steps which occur during SCR in H-form zeolites. Indeed, Li and Armor (10), in their studies on Ga-H-ZSM-5 using CH_4 as

0021-9517/97 $25.00

a reducing agent, suggest that "possibly, the role of gallium is to enhance the activation of CH_4 with the NO reduction occurring on the H^+ sites, or vice versa." Thus, a clearer understanding of the reaction mechanism of NO_x reduction on H-form zeolites may prove valuable in the development of more active metal-exchanged zeolite catalysts.

Kiovsky *et al.* (2) performed cursory studies to determine the mechanism of NO reduction with NH_3 on an "H-mordenite" catalyst (NC-300 actually contains 8–34% Fe exchanged into H-mordenite). They observed that NO requires the presence of O_2 in order to be reduced, while NO_2 does not. Moreover, increasing the NO_2/NO ratio in the reactant stream increases the rate of NO_x reduction by NH_3. Thus, they concluded that NO_2 is the reactive intermediate and that differences in SCR activity of zeolites are due to different rates at which the catalysts oxidize NO to NO_2. In analyzing the data of Kiovsky and co-workers, Marangozis (11) noticed that NO_2 was not detected in the product gas stream, but small amounts of N_2O were. Thus, he suggests that N_2O formation from adsorbed NO and adsorbed O_2 could be the rate-limiting step.

Ito and co-workers (12), who compared the activity of CeNa-mordenite to H-mordenite, suggested two possible reaction schemes. The first involves the NO_2 intermediate mechanism as described by Kiovsky and co-workers. This mechanism could explain the enhanced activity of CeNa-mordenite over LaNa-mordenite in view of their different activities for oxidizing NO to NO_2. The second scheme involves a nitrosation reaction. In this scheme, a strong oxidant (such as Ce^{IV}) could oxidize NO to a nitrosonium ion, NO^+, which reacts readily with NH_3 to form N_2. O_2 is necessary in this scheme to regenerate the active sites (Ce^{III} to Ce^{IV}). Since O_2 is involved in a different reaction step in each of these schemes (i.e., either in the initial step to oxidize NO to NO_2 or in the final step to reoxidize Ce^{III} to Ce^{IV}), Ito and co-workers designed experiments to observe transient behavior under various oxidizing conditions. In a first test, they flowed 465 ppm NO and 465 ppm NH_3 over a preoxidized CeNa-mordenite catalyst at 306°C. Initially, they observed a large decrease in NO concentration which lasted only 1 min (which they attributed to either a sudden reaction or adsorption of NO) before decreasing rapidly. They concluded that the low steady-state conversion supported their first scheme in which O_2 is required for NO oxidation (i.e., insufficient O_2 is available to maintain NO oxidation since the preoxidation step caused only the formation of Ce^{IV}). The same test performed at 510°C yielded significantly different results. The period of initially high NO conversion lasted for almost 45 min before decreasing to a low steady-state value. Integration of the conversion curve to determine the amount of NO removed (above the steady-state value) revealed a turnover number very close to 1. Thus, they concluded that at high temperatures each Ce^{IV} site is capable of oxidizing one NO atom to NO^+.

Andersson *et al.* (13) and Brandin *et al.* (6), in their studies of SCR with NH_3 over H-mordenite, observed optimal SCR activity for NO_2/NO ratios close to 1. Suspecting the possible role of NO_2 as an active intermediate, they performed experiments to correlate NO oxidation and NO_x reduction activities of Cu-mordenite and H-mordenite catalysts. Based on their negative correlation, they concluded that "an ideal NO_x reduction catalyst is a selective oxidation catalyst that cannot oxidize NO to NO_2." Infrared studies documented by Andersson *et al.* (13) and Odenbrand *et al.* (14), however, indicate a correlation between adsorbance of NO^+ species and first order reaction rate constants. Thus, they proposed an NO reduction mechanism, much like that of Ito and co-workers, involving ionized species such as adsorbed NO^+ and NO_2^-. According to this mechanism, O_2 oxidizes NO to form NO^+ and O_2^-. In NO_x mixtures, NO_2, which has a higher electron affinity than O_2, oxidizes NO resulting in the formation of NO^+ and NO_2^-. These ionization steps could explain enhanced SCR activity as NO_2/NO ratios increase to unity. The mechanism is similar to zeolite hydroxylation in which H_2O separates into H^+ and OH^- ions. In the case of NO oxidation, NO^+ species could be bonded to oxygen ions in the framework of the zeolite before reacting with adsorbed NH_3.

While previous kinetic studies provide some insights and propose possible reaction intermediates and paths, they do not provide a clear view or consensus regarding the mechanism of NO reduction. Definitive evidence to support any of the proposed mechanisms or intermediates is lacking.

In view of the potential benefits of understanding SCR reaction mechanisms on H-form zeolites and the considerable interest in ZSM-5-based catalysts, this study of NO reduction with NH_3 over H-ZSM-5 was undertaken. In particular, this study focused on the kinetics and mechanism of NO reduction with NH_3 over H-ZSM-5 (which appears to be similar to the mechanism of NO reduction over H-mordenite as presented in Eng and Bartholomew (15)). Steady-state kinetic experiments were performed to understand the rate dependence on NO, O_2, NH_3, and H_2O concentrations in the overall reaction. These tests were accompanied by transient analyses to further clarify mechanistic features of the overall reaction process.

EXPERIMENTAL

Samples of NH_4-Z-12 were obtained from Tosoh USA, and samples of H-Z-21, Na-Z-26, Na-Z-35, Na-M-5, and NH_4-M-10 (where Z and M refer to ZSM-5 and mordenite, respectively, and the last number in each sample denotes the Si/Al ratio) were obtained from PQ Corporation. Samples obtained in the Na-form were first calcined in air at 500°C for 20 h to remove any residual hydrocarbon template. They were then ion exchanged in an agitated 2 *M* ammonium acetate solution at 90°C for 5.5 h, followed by filtering and

washing with deionized, distilled water. This ion-exchange process was repeated, followed by drying overnight at 110°C to produce NH_4-form samples. NH_4-form samples were converted to H-form zeolites by heating at 3°C/min to 500°C and then holding the samples at this temperature for 1 h. Prior to testing, several samples were also pretreated in flowing He for 1 h at 500°C; however, it was determined that this pretreatment did not affect SCR activity.

Steady-state tests were performed at near atmospheric pressure (85.7 kPa) using NO (1000 to 6000 ppm), O_2 (1 to 6%), NH_3 (1000 to 6000 ppm), and H_2O (0 to 20%) in He at temperatures ranging from 330 to 430°C at GHSVs greater than 30,000. NO, NO_2 (calibration quality Matheson Gas diluted in He), and NH_3 (calibration quality Matheson Gas diluted in He) were introduced without further purification. Ultra-high-purity He was further purified using Cu-deoxo and molecular sieve traps. O_2 (10.3% in He from Matheson Gas or 100% from Whitmore Oxygen Co.) was also dried through a molecular sieve trap.

Two sets of apparatus were used to obtain kinetic data. For tests with either 10 or 20% H_2O, a fixed-bed steady-state microreactor system was utilized. It consisted of only one flowpath and contained rotameters and needle valves for setting and monitoring individual flowrates of O_2, NO, NH_3, and He. After the rotameters, O_2 and He lines were connected and the gases were passed through a controlled temperature water bath to introduce desired levels of H_2O. The humidified gases were then passed through heat-traced stainless steel lines to mix with NO and NH_3 before entry into a quartz reactor. Following the reactor, the effluent gases were passed through a 0°C condensor to remove water and NH_3. Analyses of the gases leaving the condensor were performed using an HP 5810 gas chromatograph equipped with a thermal conductivity detector and a continuous Rosemount chemiluminescence NO_x analyzer.

For temperature-programmed ammonia desorption (TPAD) and steady-state and transient tests without reactant water, the experimental apparatus shown in Fig. 1 was employed. Gases were metered using Brooks 5850 mass flow controllers. He, NO, and NH_3 were mixed in either of two stainless steel flowpaths, which enabled purging of lines with He for instantaneous changes during transient tests, and O_2 was added just prior to entry into a 0.25-inch-diameter quartz reactor. The late addition of O_2 was included to minimize potential NO_x oxidation reactions in the gas phase or catalyzed by stainless steel surfaces (16). Immediately following the reactor, a small stream of the product gases was diverted into a UTI 100C quadrapole mass spectrometer for analysis. The stream was introduced to the mass spectrometer through a two-stage pressure reduction process. Portions of product gas samples were directed from atmospheric pressure to a first stage pressure of 0.30 Torr. A sample of the gas in the first stage was diverted into the quadrapole mass spectrometer in which analysis was performed at 3.00×10^{-6} Torr.

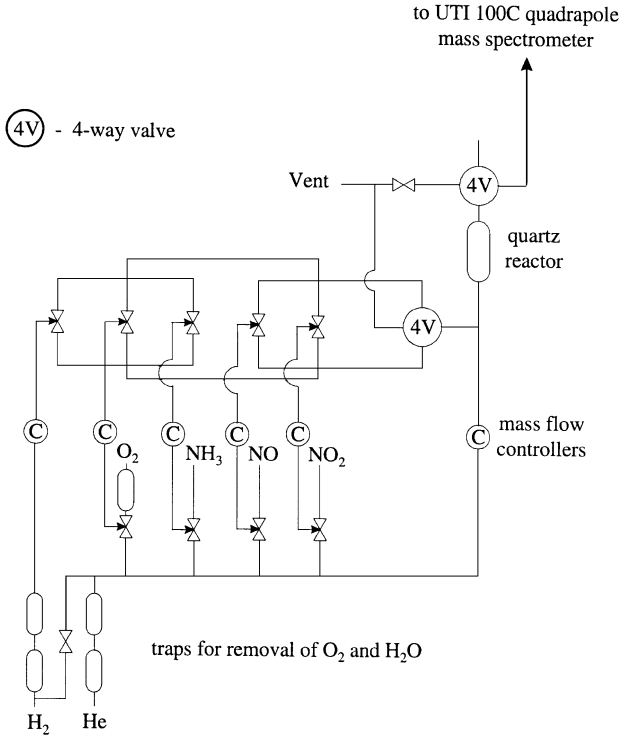

FIG. 1. Flow schematic of temperature-programmed desorption/reaction apparatus.

TPAD tests were performed by adsorbing NH_3 (3068 ppm NH_3 in He) onto approximately 100 mg samples for 1 h at 200°C. Weakly adsorbed NH_3 was desorbed by flushing in He at 200°C for 1.5 h. Repeated tests performed by varying the adsorption times and temperatures indicated these conditions to be optimum for obtaining reproducible results. Temperature-programmed desorption (TPD) was carried out by heating the samples in 100 cm^3/min He from room temperature at a rate of 11°C/min to temperatures above 600°C. Peaks at 16 and 17 amu were monitored continuously throughout the TPD ramping process.

RESULTS

Activity tests. Figure 2 compares NO conversions obtained over each of the H-form zeolites tested at standard conditions of 1000 ppm NO, 1000 ppm NH_3, 2% O_2, and GHSV = 30,000. Activities of H-M-5, H-Z-12, H-Z–21, and H-Z-26 are measurable above 350–400°C, while NO conversions of 50–60% are observed at 500°C. However, activities of H-M-10 and H-Z-35 are not significant at temperatures as high as 500°C. This result is somewhat unexpected, as it has been suggested that SCR activity is proportional to the number of acid sites present in the zeolite (13).

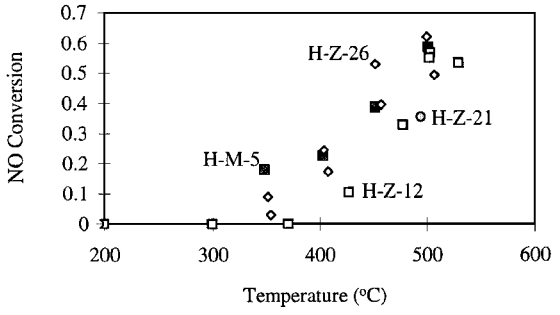

FIG. 2. Comparison of NO conversions obtained over H-mordenite and H-ZSM-5 at a GHSV of 30,000 h^{-1} in a reactant stream containing 1000 ppm NO, 1000 ppm NH_3, and 2% O_2 (conversions for H-Z-35 and H-M-10 are not shown, since they were less than 5% at temperatures exceeding 500°C).

TABLE 1

Results of Temperature-Programmed Ammonia Desorption Experiments

Zeolite[a]	Mass (g)	Al content[b] (10^{-6} mol)	Desorbed NH_3 (10^{-6} mol)	NH_3/Al ratio
H-M-5	0.107	283	200	0.71
H-M-10	0.101	153	119	0.78
H-Z-12	0.105	134	87	0.65
H-Z-21	0.101	76.1	52	0.68
H-Z-26	0.108	66.1	40	0.61
H-Z-35	0.101	46.8	34	0.74

[a] H-M-*xx* and H-Z-*xx* refer to H-mordenite and H-ZSM-5, respectively, where *xx* is Si/Al ratio determined by chemical analysis.

[b] As calculated from the Si/Al ratios reported by suppliers.

Temperature-programmed desorption tests. Concentrations of acid sites in each of the zeolites were measured using temperature-programmed NH_3 desorption (TPAD). Peak maxima are observed for H-ZSM-5 at temperatures between 440 and 500°C, while a peak maximum between 500 and 600°C is observed for H-mordenite samples. Quantities of adsorbed NH_3 can be calculated from TPAD profiles by integrating the areas under each of the large TPAD peaks. Since NH_3 concentration profiles, shown in Fig. 3, did not return to baseline values, quantities of adsorbed NH_3 were calculated by doubling integrated areas up to the peak maximum. Desorbed NH_3 concentrations are listed in Table 1. Comparisons between Figs. 2 and 3 and the data listed in Table 1 indicate that the most active zeolite of each type (H-M or H-Z) contains the highest concentration of acid sites or lowest Si/Al ratio. Thus, the number of acid sites is an important factor in determining NO SCR activity.

Similar TPD tests to observe NO_x adsorption were also performed. For example, NO adsorption was carried out by exposing H-Z-26 to 2995 ppm NO in He at 200°C for 30 min, followed by desorption in He at 200°C for 20 min. Subsequent TPD to above 500°C indicated that no NO had adsorbed. Similarly, adsorption of NO (or NO_2 through NO oxidation) in the presence of O_2 was attempted by exposing H-Z-26 to 1000 ppm NO and 2% O_2 in He for 30 min at 200°C. In this case, after 10 min of desorption in He at 200°C no adsorbed species were detected. Thus, at typical reaction temperatures, neither NO or NO_2 adsorbs strongly in H-ZSM-5. These results are consistent with results of Adelman *et al.* (17) who observed little or no adsorption of NO on H-ZSM-5. However, Adelman and co-workers did observe NO_2 adsorption, but their observed NO_2 desorption peak maximum occurs at a temperature of 80°C with very little additional NO_2 desorption at temperatures above 200°C.

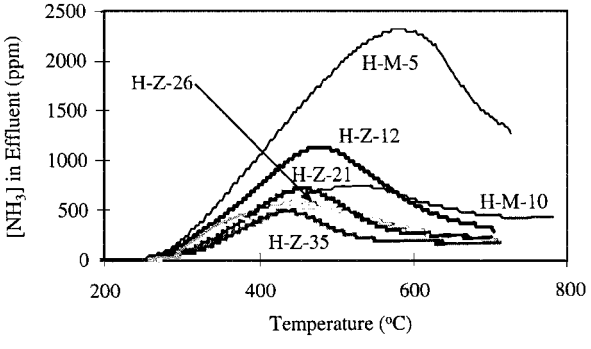

FIG. 3. Ammonia TPD profiles (heating rate of 11°C/min) for H-form zeolites after NH_3 adsorption at 200°C.

As a further test for NO_x adsorption, H-Z-26 was exposed to a flowing gas mixture containing 1000 ppm NO and 2% O_2 at 400°C for 30 min. The presence of adsorbed active species was then tested by flowing 3068 ppm NH_3 in He over the sample at the same temperature. Consistent with results of the NO_x TPD tests, no N_2 or NO desorption peaks were detected.

Kinetic tests. Kinetic tests were performed on H-Z-12, one of the most active zeolites tested. Two sets of experiments were performed, one with and one without water in the reactant gas stream. Since results of these studies were intended for applications involving high NO_x concentrations (approximately 4000 ppm NO_x), kinetic tests were performed with NO and NH_3 concentrations of 1000 to 6000 ppm, O_2 concentrations of 1 to 6% and H_2O concentrations of 0, 10, or 20%. Data obtained from the two sets of experiments were compared based upon N_2 formation rates calculated assuming differential reaction conditions (i.e., using only data with NO conversions below 20%). From data collected with 20% H_2O present (Fig. 4), an activation energy of 60.7 ± 5.6 kJ/mol for N_2 formation was determined for the reaction of 4000 ppm NO, 4000 ppm NH_3, and 4% O_2 over H-Z-12 at temperatures between 380 and 440°C.

Calculation of the standard deviation for the activation energy was performed using a Monte Carlo approach. By

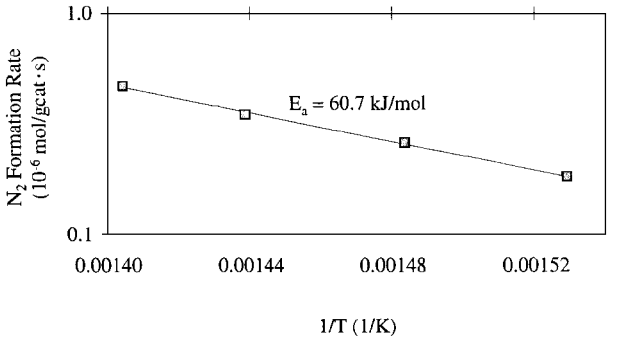

FIG. 4. Arrhenius plot of steady-state N_2 production rate for SCR on H-Z-12 in a reactant stream containing 4000 ppm NO, 4000 ppm NH_3, 4% O_2, and 20% H_2O.

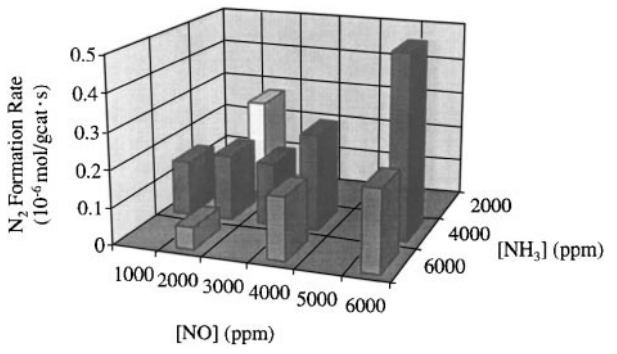

FIG. 6. Results of steady-state SCR kinetic tests for H-Z-12 at 403°C in 4% O_2 (no water in reactants).

randomly assigning fluctuations to each of the experimental parameters (i.e., individual gas flow rates, temperatures, and N_2 measurements) within the error tolerances estimated from flow and analytical instrument calibrations, numerous values of activation energy were calculated. The values reported are the mean and standard deviation of 1000 such calculations.

Rate measurements were conducted over wide ranges of reactant concentrations to determine NO and NH_3 concentration dependencies on N_2 formation rates in the presence of H_2O. As shown in Fig. 5, N_2 formation rates at 400°C (4% O_2 and 10 or 20% H_2O) increase with increasing NO concentration and decrease with increasing NH_3 concentration. The dependency on NO concentration is consistent with previous experimental reports; however, the inverse dependency on NH_3 concentration was unanticipated. For conventional SCR catalysts, such as V_2O_5, a positive order in NH_3 concentration has been reported. For instance, in studying the mechanism of NO reduction with NH_3 in excess air over V_2O_5 catalysts, Topsoe and co-workers (18) deduced a mechanism involving adsorbed (and subsequently activated) NH_3 and gaseous or weakly adsorbed NO, which is consistent with positive reaction rate orders for both NO and NH_3. Thus, the negative reaction rate order for NH_3 observed with H-ZSM-5 indicates an inhibiting influence of NH_3, despite its importance as a reducing agent.

Similar kinetic tests were performed in the absence of H_2O at 403°C (Fig. 6). The magnitude of N_2 formation rates at 400°C in the absence of H_2O (0.05 to 0.45×10^{-6} mol N_2/gcat · s) are comparable to those obtained from experiments performed with H_2O present (0.1 to 0.4×10^{-6} mol N_2/gcat · s). Furthermore, the concentration dependencies are comparable to those observed when H_2O is present in the reactant stream. Thus, H_2O does not affect N_2 formation rate under these conditions. From additional data obtained at lower NO/NH_3 ratios, it also appears that N_2 formation rates are independent of NO concentration below NO/NH_3 ratios of approximately 1.0. While this observation has not been investigated further, it is possible that N_2 formation of low NO/NH_3 ratios is derived from conversion of excess NH_3 (possibly through NH_3 oxidation to NO) since it has been observed that small amounts of N_2 can be formed when reacting NH_3 and O_2 over H-ZSM-5.

Similar trends in concentration dependence are also evident as the reaction temperature is increased to 425°C (Fig. 7). The reaction rate orders are similar for NO and NH_3 at NO/NH_3 ratios above 1.0, while at lower NO/NH_3

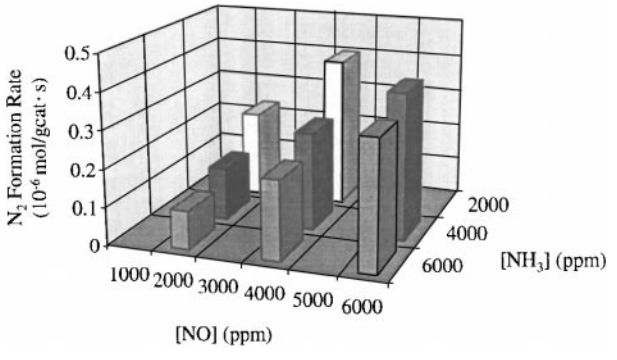

FIG. 5. Results of steady-state SCR kinetic tests for H-Z-12 at 400°C in 4% O_2, and 10 or 20% H_2O.

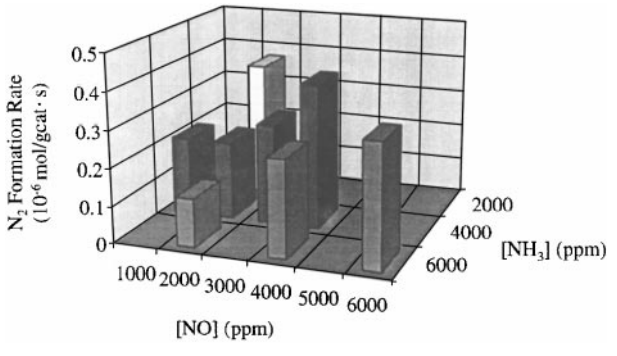

FIG. 7. Results of steady-state SCR kinetic tests for H-Z-12 at 425°C in 4% O_2 (no water in reactants).

TABLE 2

N_2 Formation Rate Data Obtained for SCR over H-Z-12 in the Presence of Water (4% O_2)

T (°C)	W_{cat} (gcat)	Q (cm^3/min)	[NO] (ppm)	[NH_3] (ppm)	[H_2O] (%)	GHSV (1/h)	Effluent [N_2] (ppm)	N_2 formation rate (10^{-6} mol/gcat · s)
380	0.416	670	3982	3982	20.4	40801	195	0.183
397	0.422	673	1980	1980	10.9	40404	221	0.205
398	0.422	675	1975	5925	21.0	40506	110	0.102
399	0.422	662	4031	6046	9.3	39696	258	0.235
399	0.422	668	4012	4012	19.8	40062	273	0.250
399	0.422	684	1950	1950	22.0	41022	245	0.230
399	0.422	666	2002	4004	9.9	39960	148	0.135
400	0.422	671	5959	5959	10.6	40278	366	0.338
400	0.422	666	4005	2002	19.9	39954	440	0.403
400	0.422	661	4037	6055	19.3	39636	226	0.206
400	0.422	666	4006	4006	9.9	39936	284	0.260
400	0.422	665	4008	2004	9.8	39918	333	0.304
400	0.422	664	2007	6021	9.7	39858	135	0.123
401	0.416	668	3993	3993	20.1	40691	279	0.260
401	0.424	673	2971	2971	20.8	40196	221	0.203
403	0.422	666	6007	4005	19.9	39954	431	0.394
420	0.422	666	6010	6010	9.8	39930	408	0.374
420	0.422	667	3996	5994	10.1	40044	286	0.262
420	0.422	731	3646	3646	18.0	43884	346	0.348
420	0.422	675	1975	5925	21.0	40506	147	0.136
420	0.422	664	2007	6021	9.7	39858	177	0.161
420	0.422	667	2000	2000	10.0	40008	247	0.226
420	0.422	669	1993	3985	10.3	40152	173	0.159
421	0.416	668	1995	3991	20.2	40709	237	0.221
421	0.424	673	2971	2971	20.8	40196	261	0.240
421	0.422	666	6007	4005	19.9	39954	519	0.475
422	0.416	668	3993	3993	20.1	40691	374	0.349
439	0.416	667	3993	3993	20.1	40618	506	0.471

ratios, N_2 formation rate is independent of NO concentration.

In view of the similarity of results obtained both with and without H_2O as a reactant (Tables 2 and 3), all data with NO/NH_3 ratios equal to or greater than 1.0 were regressed to determine reaction rate orders for each of the reactants. A Monte Carlo error analysis with 1000 iterations combined with this linear regression yielded reaction rate orders for NO, O_2, and NH_3 of 0.73 ± 0.08, 1.06 ± 0.06, and -0.61 ± 0.08, respectively. Graphical verification of the accuracy of the regression is evident in Fig. 8. By plotting calculated reaction rate constants (i.e., $k = r_{N_2}/[NO]^{0.73}[O_2]^{1.06}[NH_3]^{-0.61}$) against inverse temperature on a semilog basis, the slope of the resultant graph is proportional to activation energy. From this slope (averaged over 1000 Monte Carlo iterations), an activation energy of 60.6 ± 2.3 kJ/mol was evaluated for N_2 formation. This is in excellent agreement with the value of 60.7 kJ/mol obtained with H_2O as a reactant (Fig. 4). This value agrees well with that of 58 kJ/mol reported by Andersson *et al.* (13) for a commercial H-mordenite catalyst (Zeolon 900 H). Nam and co-workers (5) also reported a similar value of 54.0 kJ/mol for Cu-H-mordenite and H-mordenite.

Transient tests. Transient tests were conducted to further investigate the mechanism by which SCR occurs over H-ZSM-5. These transient tests were initiated in light of curious behavior observed at the end of steady-state activity tests of each active H-ZSM-5 and H-mordenite sample, i.e., a sudden decrease in NO concentration accompanied by a concurrent increase in N_2 concentration as the

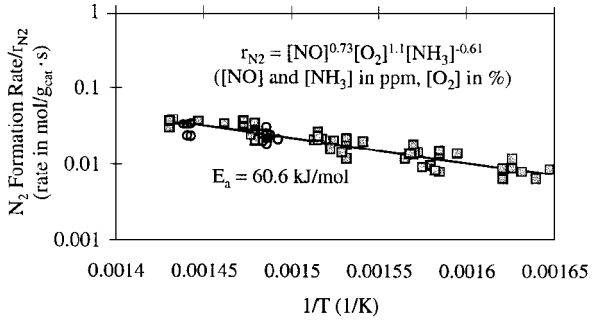

FIG. 8. Correlation plot of steady-state SCR kinetic data (NO/$NH_3 > 1$ and GHSV = 27,000 h^{-1}) for H-Z-12 with regressed rate expression. Squares indicate data for runs without H_2O in the feed and circles indicate runs with 10 or 20% H_2O.

TABLE 3

N_2 Formation Rate Data Obtained for SCR over H-Z-12 without Water ($W_{cat} = 0.0932$ g)

T (°C)	Q (cm^3/min)	[NO] (ppm)	[NH_3] (ppm)	[O_2] (%)	GHSV (1/h)	Effluent [N_2] (ppm)	N_2 formation rate (10^{-6} mol/gcat · s)
337	147	5000	5000	3	39990	57	0.052
340	147	4000	4000	2	39990	45	0.041
342	101	1000	1000	2	27404	63	0.039
342	101	4000	4000	4	27404	200	0.125
344	101	2000	2000	4	27404	140	0.087
344	147	4000	2000	2	39990	57	0.052
354	101	4000	4000	4	27404	239	0.149
358	147	2000	2000	4	39990	143	0.130
358	146	6000	6000	4	39692	98	0.088
358	147	6000	4000	4	39990	243	0.221
359	147	4000	4000	4	39990	96	0.088
360	147	5000	5000	3	39990	86	0.079
362	101	1000	1000	1	27404	31	0.019
363	101	1000	1000	2	27404	102	0.064
364	101	1000	1000	2	27404	96	0.060
364	101	4000	4000	4	27404	308	0.192
365	101	2000	2000	4	27404	221	0.138
366	147	4000	2000	2	39990	107	0.098
376	101	4000	4000	4	27404	339	0.212
380	147	2000	2000	4	39990	199	0.182
380	146	6000	6000	4	39692	146	0.132
380	147	6000	4000	4	39990	342	0.311
381	147	4000	4000	4	39990	167	0.152
383	147	5000	5000	3	39990	177	0.162
384	147	6000	6000	1	39990	44	0.040
386	101	1000	1000	2	27404	148	0.092
387	101	4000	4000	4	27404	447	0.279
387	101	4000	4000	4	27404	401	0.250
387	101	2000	2000	4	27404	337	0.210
388	147	4000	2000	2	39990	184	0.167
400	147	4000	4000	2	39990	124	0.113
403	147	2000	2000	4	39990	299	0.272
403	146	6000	6000	4	39692	246	0.223
403	147	6000	4000	4	39990	548	0.499
404	147	4000	4000	4	39990	280	0.255
406	147	5000	5000	3	39990	267	0.243
406	147	6000	6000	1	39990	103	0.094
411	147	4000	2000	2	39990	296	0.270
418	101	1000	1000	1	27404	123	0.077
425	147	2000	2000	4	39990	409	0.373
426	147	4000	4000	4	39990	431	0.393
426	146	6000	6000	4	39692	368	0.333

reaction temperature was reduced from 500 to 300°C (see Fig. 9). The sudden decrease in NO concentration was surmised to be due to either very fast reactions resulting in the consumption of NO or a temporary increase in adsorption of NO. Similarly, the increase in N_2 concentration was postulated to be due to either an increase in reaction rates resulting in additional N_2 formation or an evolution of adsorbed N_2. Since no evidence was available to distinguish between these different possibilities, additional transient tests were performed.

Beginning with steady-state operation under standard conditions of 1000 ppm NO, 1000 ppm NH_3, and 2% O_2 in He at 500°C over an H-Z-12 sample (GHSV = 30,000), the role of NO was investigated by suddenly discontinuing and then reintroducing NO, while keeping the O_2 and NH_3 concentrations constant. As shown in Fig. 10, when NO flow is discontinued at 500°C, a substantial drop in N_2 concentration immediately follows, confirming that the majority of N_2 formed originates from reaction of NO with NH_3 rather than NH_3 oxidation. NH_3 oxidation, however, does appear to contribute slightly to the formation of N_2 and NO at high temperatures, as evidenced by small decreases in N_2 and NO concentrations as temperature decreases from 500 to 200°C. Nevertheless, the amount of N_2 formed from NH_3

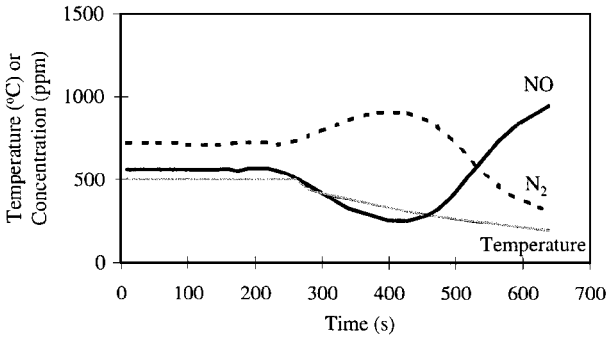

FIG. 9. Changes in NO and N_2 concentrations with time in response to a temperature decrease from 500°C during SCR over H-Z-12 in a reactant stream containing 1000 ppm NO, 1000 ppm NH_3, and 2% O_2.

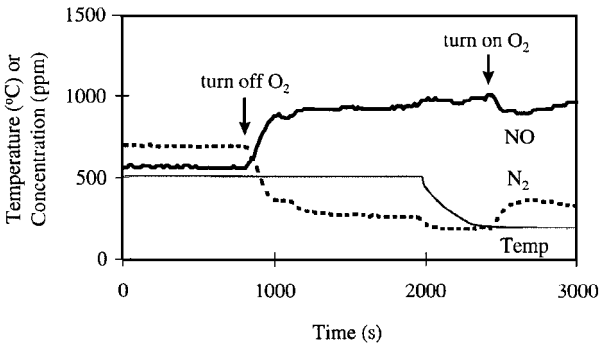

FIG. 11. Changes in NO and N_2 concentrations with time in response to changes in O_2 concentration during SCR over H-Z-12 in a reactant stream containing 1000 ppm NO, 1000 ppm NH_3, and 2% O_2 (unless otherwise noted).

oxidation is orders of magnitude smaller than that formed by SCR of NO. When NO is reintroduced at 200°C, the NO concentration monotonically increases to 1000 ppm while the N_2 concentration increases slightly (likely due to N_2 impurity in the NO tank), indicating the low activity of the catalyst at low temperatures.

A similar test (i.e., starting with the same steady-state conditions at 500°C), discontinuing O_2 instead of NO, results in an immediate reduction in N_2 formation and concomitant NO concentration increase (Fig. 11). Moreover, in the absence of O_2, no sudden decrease in NO concentration occurs at the end of steady-state activity tests as temperature is reduced. Thus, it is clear that O_2 is necessary for NO to react both at steady-state and during temperature changes.

Another transient test was performed to further clarify the roles of NO and O_2 in the SCR process. In this test (Fig. 12), NH_3 was first adsorbed onto a sample of H-Z-26 at 400°C and then the sample was flushed with He. Figure 12 shows that as 1000 ppm NO in He is introduced to the sample (with no O_2 present), small amounts of N_2 (mostly due to N_2 impurities in the NO cylinder) and H_2O are detected which decrease as NO is discontinued. After flushing the surface briefly with He, addition of O_2 to the reactant stream (with no NO present) results in considerable H_2O formation, as expected due to reaction between O_2 and adsorbed NH_3, but negligible N_2 formation. When NO (in the absence of O_2) is then reintroduced to the dehydrogenated sample (after the reactor is flushed with He), the same small increase in N_2 concentration occurs, as observed at the beginning of this transient test. Only when both NO and O_2 simultaneously contact the sample does substantial NO disappear and N_2 appear.

The use of transient tests involving NH_3 concentration variations offers insight into the role of NH_3 in the reaction mechanism. When NH_3 is discontinued (after steady state had been established), changes in N_2 and NO concentrations (Fig. 13) are not as instantaneous as in the previous transient tests. Instead, there is an initial lag period, followed by a small increase in N_2 concentration and accompanying decrease in NO concentration before the SCR reactions cease. As temperature is decreased from 500 to 200°C, a decrease in NO concentration is again detected; however, in contrast to responses observed at the end of

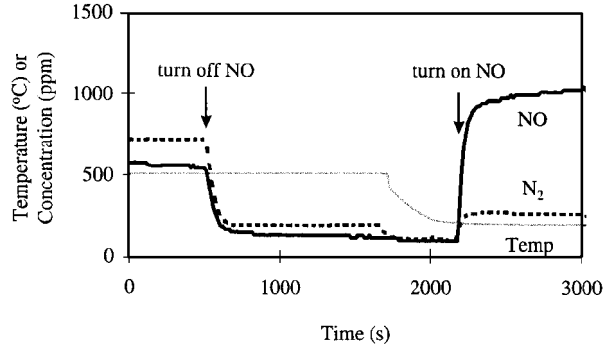

FIG. 10. Changes in NO and N_2 concentrations with time in response to changes in NO concentration during SCR over H-Z-12 in a reactant stream containing 1000 ppm NO, 1000 ppm NH_3, and 2% O_2 (unless otherwise noted).

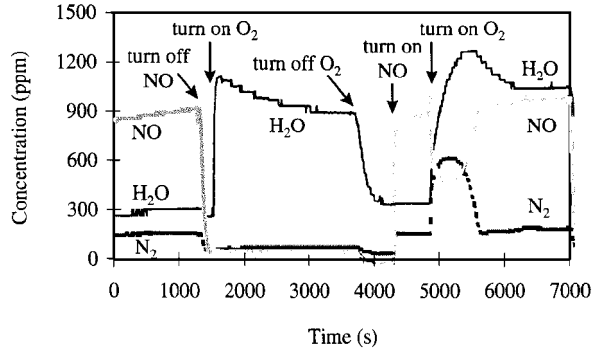

FIG. 12. Interactions between O_2, NO, and adsorbed NH_3 during SCR over NH_3-pretreated H-Z-26 in a reactant stream initially containing 1000 ppm NO in He.

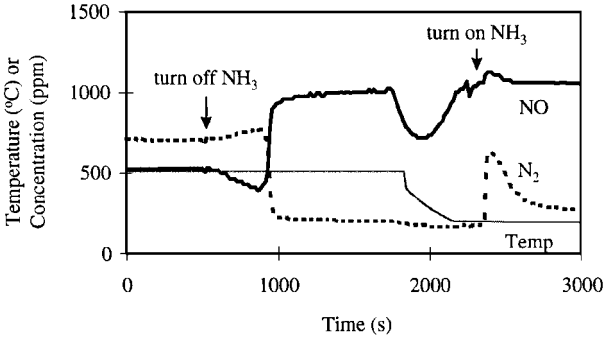

FIG. 13. Changes in NO and N_2 concentrations with time in response to changes in NH_3 concentration during SCR over H-Z-12 in a reactant stream containing 1000 ppm NO, 1000 ppm NH_3, and 2% O_2 (unless otherwise noted).

steady-state SCR tests, there is no accompanying increase in N_2 concentration coinciding with NO disappearance, but rather a large increase upon NH_3 reintroduction.

The lag period is more easily observed at higher concentrations of reactants. In a separate test, also performed with H-Z-12 ($T = 440°C$, GHSV = 76,000), the zeolite sample was exposed to 4000 ppm NH_3 in He until complete adsorption of NH_3 onto the zeolite had occurred. 4000 ppm NO and 4% O_2 were then added while maintaining the same NH_3 concentration. As shown in Fig. 14, when NH_3 flow is discontinued, no immediate reduction in NO concentration occurs. Not until NH_3 concentration begins to decrease does the decrease in NO concentration and concurrent increase in N_2 concentration occur.

DISCUSSION

The results of kinetic tests performed in this study combined with the results of transient tests provide new mechanistic insights regarding SCR of NO with NH_3 over H-ZSM-5.

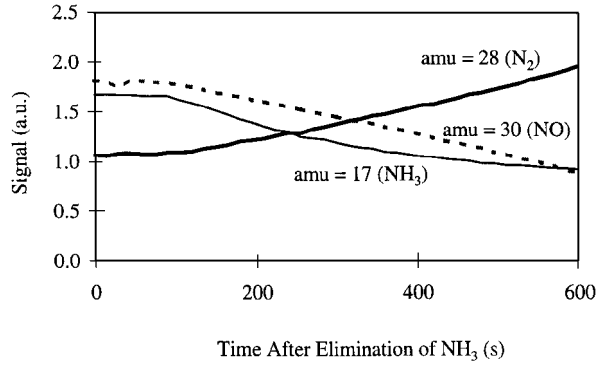

FIG. 14. Changes in NH_3, N_2, and NO concentrations (17, 28, and 30 amu) with time in response to elimination of gaseous NH_3 during SCR over H-Z-12 in a reactant stream initially containing 4000 ppm NO, 4000 ppm NH_3, and 4% O_2 at 440°C and a GHSV of 76,000 h^{-1}.

Influence of H_2O. The influence of H_2O on SCR with NH_3 over H-ZSM-5 can be inferred by comparing results of kinetic tests performed over H-Z-12 with and without H_2O as a reactant (Figs. 5 and 6). For comparable NO and NH_3 concentrations, N_2 formation rates with and without H_2O present are nearly the same (in both cases, N_2 formation rates range from 0.05×10^{-6} mol N_2/gcat · s at [NO] = 2000 ppm and [NH_3] = 6000 ppm, to approximately 0.45×10^{-6} mol N_2/gcat · s at [NO] = 6000 ppm and [NH_3] = 2000 ppm). Moreover, the excellent agreement between activation energies regressed from the two sets of data (60.7 kJ/mol with H_2O and 60.6 kJ/mol without H_2O) also suggests that H_2O does not affect SCR with NH_3 over H-ZSM-5. The reliability of the regressed correlation (Fig. 8) demonstrates the validity of the correlation for wide ranges of H_2O concentration and temperature.

Jentys *et al.* (19) discovered that Brønsted acid sites in H-ZSM-5 are the most important adsorption sites for H_2O adsorption at high H_2O concentrations. As shown in TPAD tests, these are the same sites onto which NH_3 adsorbs. The absence of H_2O inhibition during SCR of NO with NH_3 over H-ZSM-5 may therefore reflect the stronger affinity for acid sites of NH_3 over H_2O. This is consistent with results reported by Bagnasco (20) which show that H_2O displaces weakly adsorbed NH_3 in H-ZSM-5 and H-mordenite, but not NH_3 adsorbed onto stronger Brønsted acid sites. When metal cations are present, H_2O adsorbs strongly on the cations (19). Thus, for many metal-exchanged catalysts, increased affinity of H_2O to cations is likely the cause of H_2O inhibition effects.

Interactions of NO with H-zeolites, O_2, and NH_3. The kinetic data obtained in this study indicate that the rate of N_2 formation rate has a positive dependence on NO concentration (NO order is 0.73). Since transient responses to changes in NO concentration indicate that N_2 formation decreases significantly in the absence of NO and that the amount of N_2 formed due to NH_3 oxidation is small (Fig. 10), N_2 formation rates are essentially representative of NO reduction rates.

The reaction rate orders for NO and O_2 (0.73 and 1.06, respectively) are close to first order dependencies consistent with a rate-limiting step involving reaction between one NO molecule and one O_2 molecule. Gas-phase NO oxidation to NO_2 (which has been suggested as a rate-limiting step for NO reduction) involves reaction between NO and O_2 with homogeneous NO oxidation occurring via an NO dimer complex corresponding to reaction orders of 2 for NO and 1 for O_2 (21). The reaction rate orders determined for SCR over H-ZSM-5 do not appear to be consistent with a rate-limiting step involving gaseous NO oxidation to NO_2; however, since excess NH_3 also inhibits the SCR reaction and the influence of this inhibition upon reaction rate orders for NO and O_2 is unknown, it is difficult to draw definitive conclusions regarding the reaction

mechanism strictly from analysis of the steady-state kinetic data.

Results of NO adsorption tests (TPD with and without O_2 present and surface reaction tests of gaseous NH_3 with adsorbed NO_x) reveal that NO and NO_2 do not adsorb appreciably onto H-form zeolites at temperatures in excess of 200°C. However, adsorption of some NO_x species must occur during SCR. This is evident from analysis of transient responses observed after elimination of flowing NH_3 (Fig. 13) showing that as temperature is reduced from 500 to 200°C (with 1000 ppm NO and 2% O_2 flowing over H-Z-12 which previously had been exposed to NH_3), a sudden drop in NO concentration is observed. This behavior can be contrasted to responses observed when NH_3 is concurrently flowing (Fig. 9) which indicate that N_2 formation coincides with a decrease in NO concentration when sufficient NH_3 is present while temperature is decreased. This comparison suggests that in the former experiment, in which no change in N_2 concentration is observed during the decrease in temperature, NO does not react to form N_2 (or other N-containing species in any significant amounts such as NO_2 or N_2O); thus, the decrease in NO concentration as temperature decreases must be due to adsorption of NO_x species.

A nitrosation reaction involving NO oxidation to nitrosonium ions, NO^+, would be consistent with observed reaction rate orders for both NO and O_2 and may explain adsorption of NO_x species. According to Brandin and co-workers (6), such a mechanism would be enhanced by NO_2, since NO_2 is a stronger oxidant than O_2 and should increase rates of NO oxidation to NO^+. They proposed that NO^+ ions formed from NO oxidation (by O_2 or NO_2) could adsorb on framework oxygen sites.

Role of O_2. It has been suggested that O_2 functions either to oxidize NO_x species or to reoxidize sites which have undergone reduction in the SCR process. The reaction rate order of 1, determined by kinetic studies performed in this work, is consistent with either of these mechanisms, but again this steady-state result does not enable discrimination between them.

If the role of O_2 in SCR on H-ZSM-5 is similar to that occurring on V_2O_5, then NO and NH_3 react on active sites to form N_2, with O_2 serving to reoxidize the surface (18). In H-form zeolites, this reoxidation would be tantamount to H atom removal since direct reaction between one NO molecule and one NH_3 molecule to form N_2 and H_2O leaves an unreacted H atom. The results of transient responses to changes in O_2 concentration (Fig. 11) are inconclusive as there does appear to be a small amount of N_2 formed by reaction between NO and NH_3 when O_2 is not present (evidenced by small drop in N_2 concentration as temperature decreases from 500°C). Likewise, when O_2 is reintroduced, a small amount of N_2 is formed and NO disappears, which could be attributed to H atom removal by O_2 that exposes active sites to further NO reaction and/or adsorption. Analysis of the transient test depicted in Fig. 12, however, appears to discount such a mechanism. When NO was exposed (in the absence of O_2) to an H-Z-26 sample upon which NH_3 had been presorbed, only small increases in N_2 concentration were detected. (Due to reoccurrence of this baseline level of N_2 during each successive injection of NO, this increase was attributed to N_2 impurities in the NO source tank.) The fact that N_2 was not formed by reaction when NO alone was exposed to the NH_3-presorbed zeolite indicates that NO does not react directly with adsorbed NH_3 to form N_2; however, it is possible that excess H atoms inhibit NO reactions with adsorbed NH_3. In order to investigate this latter possibility, the surface was flushed with He and exposed to O_2, which resulted in considerable H_2O formation, as expected (i.e., removal of excess H atoms). The oxidized surface was then flushed with He and again exposed to NO. If the role of O_2 is merely for surface reoxidation (i.e., removal of H atoms through H_2O formation) then significant N_2 formation would be expected upon NO reintroduction to the surface. This, however, did not occur when NO was exposed to the oxidized surface. Rather, it was not until both NO and O_2 simultaneously contacted the sample that substantial N_2 formation occurred. This leads to the conclusion that NO and O_2 react in some manner to form an active species which reacts quickly with adsorbed NH_3 to form N_2.

Both the NO_2 intermediate mechanism and the nitrosation reaction mechanism (formation of NO^+) require an initial step involving reaction between NO and O_2. Thus, the transient tests involving O_2 concentration changes support these mechanisms, but do not provide sufficient evidence to distinguish which mechanism occurs in SCR.

Role of NH_3. It is apparent that NH_3 functions as a reducing agent in SCR as evidenced by the decrease in NO reduction when reactant NH_3 flow is discontinued (Fig. 13). Figures 9 and 13 illustrate that as temperature decreases from 500°C, NO species can adsorb. When NH_3 is present, N_2 is concurrently formed during this NO adsorption period (Fig. 9), but when NH_3 is not present, N_2 is not formed (Fig. 13). In the latter situation, when NH_3 is reintroduced an increase in N_2 concentration occurs (Fig. 13). From TPAD tests, it is also evident that NH_3 adsorbs strongly onto acid sites in zeolites. Thus, NH_3 is necessary for NO reduction to occur and NH_3 adsorption onto acid sites is likely a necessary step in the overall reaction mechanism.

From kinetic tests, however, a negative reaction rate order is observed for gas-phase NH_3, suggesting that it also inhibits the reaction in some manner (see Figs. 13 and 14). Figures 13 and 14 illustrate the responses in NO and N_2 concentrations to changes in NH_3 concentration. In particular, it can be seen that the response to discontinuing NH_3 flow is not immediate, but coincides with a decrease in gas-phase NH_3 concentration. As gas-phase NH_3 concentration decreases, NO disappears while N_2 forms. The fact that

NO and N_2 concentrations do not change until gas-phase NH_3 concentration diminishes suggests that gaseous NH_3 inhibits adsorption of the active NO_x species. This conclusion is further supported by the higher conversion observed in the absence of gaseous NH_3 as shown in Fig. 12. That is, when NO and O_2 contact an H-Z-26 sample which has been presorbed with NH_3 (and flushed of excess NH_3), peak conversions reaching 50% are observed at 288°C. In comparison, for a comparable temperature and GHSV, a steady-state conversion of only 20% is achieved when NH_3 is simultaneously injected with the other reactant gases (Fig. 2). Both the transient response to decreases in NH_3 concentration and the enhanced NO conversion observed when gas-phase NH_3 is eliminated suggest that gas-phase NH_3 inhibits NO reduction. Since molecular NH_3 can bond with surface NH_4^+ (22), it is possible this inhibition effect arises when excess NH_3 surrounds NH_4^+ (adsorbed NH_3) preventing NO_x diffusion to the active, adsorbed NH_3 species.

Despite the inhibiting effect of NH_3 on NO_x adsorption, prior exposure to NH_3 appears to be necessary for NO_x adsorption to occur. Results of tests in which H-Z-26 was exposed to NO (with or without O_2), followed by temperature-programmed desorption or reaction with gaseous NH_3, indicate that no NO_x species adsorb directly onto H-Z-26. In contrast, Fig. 9 indicates adsorption of some type of active NO_x species during SCR as temperature is decreased (as discussed previously). In each of the transient tests which showed evidence of NO_x adsorption, NH_3 had been adsorbed onto the zeolite. In the test involving transient responses to changes in gas-phase NH_3 concentration (Fig. 13), NO adsorption occurred under slightly different conditions. Just prior to the decrease in temperature (during which time NO adsorption was observed), NO reduction was negligible, which suggests that all active, adsorbed NH_3 had been depleted by this time. Despite the absence of adsorbed NH_3, NO could still adsorb as temperature decreased and subsequently react when NH_3 was reintroduced. Since NO adsorption can occur in zeolites when chemisorbed NH_3 is present or when NH_3 had recently been exposed to the zeolite, it is possible that NH_3 adsorption induces some type of change in the zeolite that facilitates NO_x adsorption (e.g., leaves unreacted hydrogen behind which can bond with NO_x).

Role of acid sites. The affinity of acid sites within H-mordenite and H-ZSM-5 for NH_3 is well documented (23–26). Other than providing sites for NH_3 adsorption, however, it is not clear what other roles, if any, these acid sites have in SCR. Andersson *et al.* (13) performed SCR tests on a series of acid-leached dealuminated H-mordenite samples ranging from a Si/Al ratio of 5.3 to 9.9 and found the SCR activity of their catalysts to be proportional to Al content. They further concluded that Lewis acid sites, which are either metal cations or dehydroxylated Brønsted acid sites, are the active sites for NO_x reduction. Results observed in this study, however, do not indicate a direct correlation between Al content and SCR activity. Indeed, results depicted in Fig. 2 show that a minimum Al content (or maximum Si/Al ratio) exists, below which SCR activity is negligible. In the case of H-mordenite, H-M-5 exhibits considerable SCR activity, while H-M-10 does not. Similarly, H-Z-12, H-Z-21, and H-Z-26 are active, while H-Z-35 is not.

Analysis of the tetrahedral sites (T-sites) present in ZSM-5 indicates that each T-site is bonded to framework oxygen atoms which are exposed in 5.1- to 5.5-Å pore channels (either straight pore channels in the [010] direction or sinusoidal channels interconnecting the straight channels). Furthermore, results of computer simulations (27–29) suggest that Brønsted acid sites (arising from Al substitution in T-sites) are randomly distributed in ZSM-5 and exhibit uniform strength (23, 30). Thus, all Al atoms in H-ZSM-5 should theoretically produce Brønsted acid sites of comparable strength which are accessible to small reactant molecules such as NH_3.

In view of the random distribution of acid sites of comparable strength, it is possible that the high SCR activity of H-Z-12 over H-Z-35 may be explained by consideration of the distances between neighboring acid sites in pore channels of ZSM-5. For a Si/Al ratio of 12, probability dictates that pairs of acid sites (arising from Al substitution into a T-site) will be present in many adjacent 10-membered rings, or 10-rings (Fig. 15). Since 10-rings surrounding straight pore channels in ZSM-5 are located only 2–4 Å apart in the [010] direction, neighboring acid sites in adjacent 10-rings will be located no more than approximately 7 Å apart. Considering that the N–Al distance between NH_4^+ ions bonded to oxygen atoms associated with Al T-sites is 2.9–3.0 Å (22), the separation between N atoms of neighboring adsorbed NH_3 molecules may be as low as 2–3 Å. In other words, for low Si/Al H-ZSM-5, pairs of neighboring acid sites may result in pairs of adsorbed NH_3 molecules which are close enough that other reactant molecules (such as NO or NO_2) will react or bond with both of the adsorbed NH_3 molecules. In contrast, a high Si/Al H-ZSM-5 such as H-Z-35, may not have acid sites which are sufficiently close together to enable reaction in such a manner. Thus, the high SCR activity

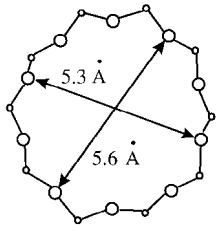

FIG. 15. 10-ring of ZSM-5 viewed along [010]. (T-sites represented by smaller circles which are connected by framework oxygen represented by larger circles.)

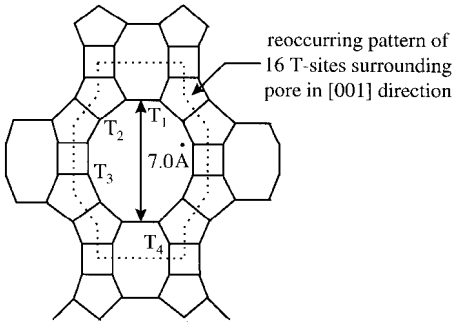

FIG. 16. 12-ring of mordenite viewed along [001] showing four types of T-sites. (Lines represent framework oxygen atoms connecting T-sites; a T-site is present at each intersection.)

of low Si/Al H-ZSM-5 zeolites, such as H-Z-12, H-Z-21, and H-Z-26, may be due to the presence of neighboring acid sites which are sufficiently close as to enable reaction between NH_3 molecules adsorbed onto a pair of acid sites (referred to as "pairs of interacting acid sites" below).

It has been documented that mordenite contains four nonequivalent T-sites (Fig. 16). Of these T-sites, T_4-sites are not bonded with framework oxygen atoms which are exposed in the 7.0 Å pore channels. Thus, Al substitution into only 75% of the T-sites of H-mordenite would produce Brønsted acid sites which are accessible to reactant molecules in the straight pore channels of mordenite. Furthermore, due to the larger diameter pores of mordenite (as compared with ZSM-5), adsorption of NH_3 onto pairs of acid sites in adjacent 12-rings may not result in adsorbed molecules which are sufficiently close so as to enable reaction between pairs of adsorbed NH_3 molecules. In view of the possible formation of inaccessible acid sites and the larger distances separating T-sites in adjacent 12-rings of mordenite, higher Al contents are necessary in mordenite as compared with ZSM-5 to ensure the formation of pairs of interacting acid sites. This may explain the SCR activity of H-M-5 and inactivity of H-M-10, even though H-ZSM-5 can exhibit SCR activity with a much higher Si/Al ratio (Si/Al = 26).

In order to reconcile the apparent contradiction between results presented by Andersson *et al.* and those presented in this study, it is important to understand how acid leaching causes dealumination. Theoretical calculations and X-ray diffraction studies suggest preferential vicinal siting of Al (i.e., pairs of Al T-sites located in second coordination spheres) in 4-rings of mordenite when high concentrations of Al are present (31, 32). When mordenite is dealuminated by acid leaching, simultaneous extraction of vicinal Al atoms occurs resulting in the formation of silanol defect sites (SiOH groups) with no evidence of residual amorphous alumina (31, 32). These same defect sites are not present in freshly prepared zeolite samples. It is possible that silanol defect sites in the dealuminated H-mordenite samples tested by Andersson and co-workers provide additional adsorption sites which are not present in H-M-10. The presence of silanol defect sites could then explain why acid-leached dealuminated H-mordenite with a Si/Al of 9.9 exhibits SCR activity while H-M-10, which does not possess silanol defect sites, does not.

The fact that Andersson and co-workers found a direct correlation between Al content and SCR activity indicates that Brønsted acid sites are the important adsorption sites in SCR. Neighboring silanol groups in dealuminated zeolites, however, may provide the additional NH_3 adsorption sites necessary when pairs of interacting Brønsted acid sites are not present.

As an extension of this investigation an NMR study is presently underway to assess the nature of framework Al, nonframework Al, and Brønsted acid sites in the same group of catalysts. Preliminary results indicate a good correlation between SCR activity and either Brønsted acidity or framework Al; however, there is no apparent correlation between nonframework Al and zeolite SCR activity.

CONCLUSIONS

A series of kinetic tests have been performed to study the mechanism by which NO reduction with NH_3 occurs over H-form zeolites. Regression of kinetic data (collected with and without H_2O present) yields an activation energy of approximately 60.6 kJ/mol. The orders of reaction, determined from these kinetic tests, for NO, O_2, and NH_3 are 0.73, 1.06, and −0.61, respectively. Combining these results with results of transient experiments leads to the following conclusions.

1. H_2O does not influence SCR with NH_3 over H-ZSM-5 at reaction temperatures above 340°C.

2. Either an NO oxidation reaction to NO_2 or a nitrosation reaction involving NO oxidation to NO^+ is consistent with experimental observations as a rate-limiting step in the reaction mechanism. Transient results indicate that the active intermediate form of NO (either NO_2 or NO^+) adsorbs during SCR reaction. In the nitrosation mechanism, NO^+ could adsorb on framework oxygen sites. From results of this study, it is unclear how NO_2 adsorbs at reaction temperatures since NO_x TPD results indicate negligible adsorption of NO_2 onto H-ZSM-5 at temperatures above 200°C.

3. The main role of O_2 is to react with NO to form an active intermediate species which can adsorb. In accordance with the reaction mechanisms proposed, O_2 oxidizes NO to either NO_2 or NO^+.

4. Adsorbed NH_3 functions as a reducing agent in SCR over H-form zeolites. However, excess gaseous NH_3 appears to inhibit the SCR reaction by limiting access of the active NO species to adsorption sites within the zeolite. It also appears that adsorbed NH_3 facilitates adsorption of the active NO_x species, since NO adsorption (with or

without O_2) does not occur at high temperatures without prior exposure of the zeolite to NH_3.

5. For freshly prepared H-form zeolites, there appears to exist a minimum Al content, below which SCR activity is negligible. Adsorption of NH_3 onto pairs of neighboring Brønsted acid sites in zeolites, such that the pairs of adsorbed NH_3 molecules are close enough together so that they can both bond with other reactant molecules, could explain this limitation. In acid-leached dealuminated zeolites, SiOH groups formed as a result of dealumination, may provide additional NH_3 adsorption sites.

ACKNOWLEDGMENTS

We gratefully acknowledge the assistance of PQ Corporation, John Armor (Air Products), and Lynn Slaugh (Shell) in providing samples of zeolites.

REFERENCES

1. Pence, D. T., and Thomas, T. R., *in* "Proceedings of the AEC Pollution Control Conference, CONF-721030," 1972, p. 115.
2. Kiovsky, J. R., Koradia, P. B., and Lim, C. T., *I.E.C. Prod. Res. Dev.* **19**, 218 (1980).
3. Seiyama, T., Arakawa, T., Matsuda, T., Yamazoe, N., and Takita, Y., *Chem. Lett.*, 781 (1975).
4. Pence, D. T., and Thomas, T. R., "An Evaluation of NO_x Abatement by NH_3 over Hydrogen Mordenite for Nuclear Fuel Reprocessing Plants," Idaho National Engineering Laboratory, Contract EY-76-C-07-1540, 1978.
5. Nam, I. S., Eldridge, J. W., and Kittrell, J. R., *Stud. Surf. Sci. Catal.* **38**, 589 (1988).
6. Brandin, J. G. M., Andersson, L. A. H., and Odenbrand, C. U., *Catal. Today* **4**, 187 (1989).
7. Ham, S. W., Choi, H., Nam, I. S., and Kim, Y. G., *Catal. Today* **11**, 611 (1992).
8. Yogo, K., Umeno, M., Watanabe, H., and Kikuchi, E., *Catal. Lett.* **19**, 131 (1993).
9. Li, Y., and Armor, J. N., *Appl. Catal. B* **2**, 239 (1993).
10. Li, Y., and Armor, J. N., *J. Catal.* **145**, 1 (1994).
11. Marangozis, J., *Ind. Eng. Chem. Res.* **31**, 987 (1992).
12. Ito, E., Hultermans, R. J., Lugt, P. M., Burgers, M. H. W., Rigutto, M. S., van Bekkum, H., and van den Bleek, C. M., *Appl. Catal. B* **4**, 95 (1994).
13. Andersson, L. A. H., Brandin, J. G. M., and Odenbrand, C. U. I., *Catal. Today* **4**, 173 (1989).
14. Odenbrand, C. U. I., Andersson, L. A. H., Brandin, J. G. M., and Haras, S., *Catal. Today* **4**, 155 (1989).
15. Eng, J., and Bartholomew, C. H., *J. Catal.* **171**, 27 (1997).
16. Peterson, E. E., Landau, J., and Saucedo, E., *in* "Catalytic Chemistry of Nitrogen Oxides" (R. L. Klimisch and J. G. Larson, Eds.), p. 119. Plenum Press, NY. 1975.
17. Adelman, B. J., Lei, G. D., and Sachtler, W. M. H., *Catal. Lett.* **28**, 119 (1994).
18. Topsoe, N. Y., Dumesic, J. A., and Topsoe, H., *J. Catal.* **151**, 241 (1995).
19. Jentys, A., Warecka, G., Derewinski, M., and Lercher, J. A., *J. Phys. Chem.* **93**, 4837 (1989).
20. Bagnasco, G., *J. Catal.* **159**, 249 (1996).
21. Brandin, J. G. M., Andersson, L. H., and Odenbrand, C. U. I., *Acta Chemica Scandinavica* **44**, 784 (1990).
22. Teunissen, E. H., van Santen, R. A., Jansen, A. P. J., and van Duijneveldt, F. B., *J. Phys. Chem.* **97**, 203 (1993).
23. Hidalgo, C. V., Itoh, H., Hattori, T., Niwa, M., and Murakami, Y., *J. Catal.* **85**, 362 (1984).
24. Karge, H. G., and Dondur, V., *J. Phys. Chem.* **94**, 765 (1990).
25. Karge, H. G., *in* "Catalysis and Adsorption by Zeolites" (G. Ohlmann *et al.*, Eds.), p. 133. Elsevier, Amsterdam, 1991.
26. Choi, E. Y., Nam, I. S., Kim, Y. G., Chung, J. S., and Lee, J. S., *J. Mol. Catal.* **69**, 247 (1991).
27. Alvarado-Swaisgood, A. E., Barr, M. K., Hay, P. J., and Redondo, A., *J. Phys. Chem.* **95**, 10031 (1991).
28. Lonsinger, S. R., Chakraborty, A. K., Theodorou, D. N., and Bell, A. T., *Catal. Lett.* **11**, 209 (1991).
29. Schröder, K. P., Sauer, J., Leslie, M., and Catlow, C. R. A., *Zeolites* **12**, 20 (1992).
30. Chen, D. T., Sharma, S. B., Filimonov, I., and Dumesic, J. A., *Catal. Lett.* **12**, 201 (1992).
31. Bodart, P., Nagy, J. B., Debras, G., Gabelica, Z., and Jacobs, P. A., *J. Phys. Chem.* **90**, 5183 (1986).
32. Miller, J. T., Hopkins, P. D., Meyers, B. L., Ray, G. J., Roginshi, R. T., Zajac, G. W., and Rosenbaum, N. H., *J. Catal.* **138**, 115 (1992).